

Supplement of A Fast Data-Driven Method for Genotype Imputation, Phasing, and Local Ancestry Inference: MendelImpute.jl

June 28, 2021

1 Supplemental Material

1.1 Imputation Quality Scores

Consider the observed genotype $x_{ij} \in [0, 2] \cup \{missing\}$ at SNP i of sample j and the corresponding imputed genotype g_{ij} derived from the two extended haplotypes of j . If S_i denotes the set of individuals with observed genotypes at the SNP, then MendelImpute's quality score q_i for the SNP is defined as

$$q_i = 1 - \frac{1}{|S_i|} \sum_{j \in S_i} \left(\frac{x_{ij} - g_{ij}}{2} \right)^2.$$

Note that $0 \leq q_i \leq 1$ and that the larger the quality score, the more confidence in the imputed values. Because q_i can only be computed for the typed SNPs, an untyped SNP is assigned the average of the quality scores for its two closest flanking typed SNPs. Figure 1A plots each SNP's quality score in the 1000G Chr20 experiment summarized in Table ???. For each sample, one can also compute the mean least squares error over all p SNPs to obtain a per-sample quality score. This is shown in Figure 1B. By default MendelImpute outputs both quality scores. Thus, investigators can perform post-imputation quality control by SNPs and by samples separately.

Empirically, it is rather common for a sample subject to harbor a few poorly imputed windows. Thus, we observe a long left tail in the histogram for per-sample error in Figure 1. Unfortunately, the bad windows generally do not exhibit any discernible regional patterns across subjects. We suspect that poorly imputed windows involve breakpoints that occur near the middle of a window. It is possible to detect such breakpoints by IBS matching and ancestry weighting [4]. We plan a detailed analysis of this issue in future work.

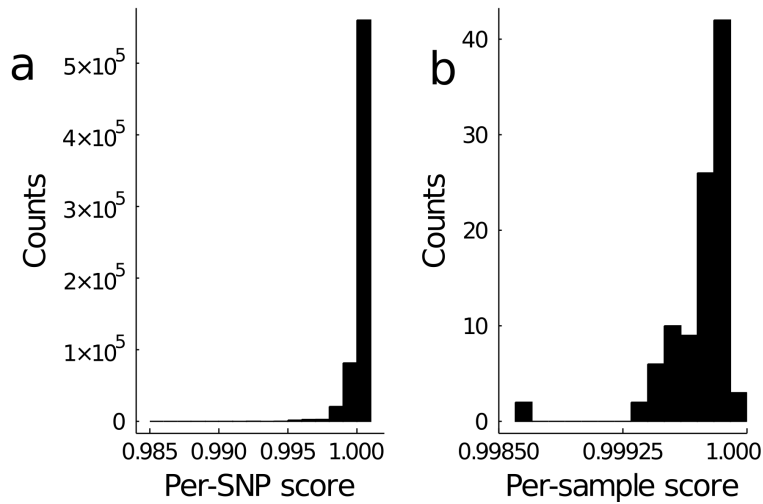


Figure 1: Histograms of per-SNP and per-sample quality scores for chromosome 20 in our 1000G analysis. By default `MendelImpute` computes (a) per-SNP quality scores and (b) per-sample quality scores. SNPs and samples with noticeably lower quality scores should be removed from downstream analysis.

22 1.2 JLSO Compressed Reference Haplotype Panels

23 The `jls0` format is constructed in three steps: (a) specify window intervals, (b) compute unique haplotypes in
 24 addition to hash maps to reference haplotypes in each window, and (c) save the result in a binary compressed
 25 format via the `JLSO.jl` package [1]. The resulting `jls0` files are 30-50x faster to read and 3-5x smaller in file
 26 size (varies depending on window width) than compressed VCF files in the `vcf.gz` format. Note the `jls0`
 27 format is simply a container object that facilitates reading and transferring large VCF files stored as Julia
 28 variables. In principle, all files that are slow to read can be pre-processed and stored in this alternative format
 29 for quicker access. As such, we similarly store ultra-compressed sample haplotypes, as discussed in Section
 30 3.4, using the `JLSO.jl` package.

31 1.2.1 Adaptive Window Widths via Recursive Bisection

32 The first step in generating JLSO haplotype panel is to specify genomic window ranges. The width of genomic
 33 windows is an important parameter determining both imputation efficiency and accuracy. Empirically, larger
 34 window widths give better error rates but also increase the computational burden of the matrix multiplications
 35 and minimum entry search described in Section 2.2. The magnitudes of these burdens depend on local hap-
 36 lotype diversity. Thus, we choose window widths dynamically. This goal is achieved by a bisection strategy.
 37 After aligning all typed SNPs with the reference panel, initially we view all typed SNPs on a large section of a
 38 chromosome as belonging to a single window. We then divide the window into equal halves if it possesses too
 39 many unique haplotypes. Each half is further bisected and so forth recursively until every window contains

40 fewer than a predetermined number of unique haplotypes. Empirically, choosing the maximum number d_{max}
41 of unique haplotypes per window to be 1000 works well for both real and simulated data. When a larger
42 number is preferred, we resort to a stepwise search heuristic for minimizing criterion (??) that scales linearly
43 in the number of unique haplotypes d . This heuristic is described above.

44 **1.2.2 Elimination of Redundant Haplotypes by Hashing**

45 Within a small genomic window of the reference panel, multiple haplotype pairs may be identical at the
46 typed SNPs. Only the unique haplotypes play a role in matching reference haplotypes to sample genotypes.
47 MendelImpute identifies redundant haplotypes by hashing. For each reference haplotype limited to the win-
48 dow, hashing stores an integer representation of the haplotype via a hash function. This integer serves as an
49 index (key) to locate the reference haplotype (value). Put another way, hashing stores the inverse images of
50 the map from reference haplotypes to unique haplotypes. In our software, the `GroupSlices.jl` package [2]
51 identifies a unique key for each haplotype.

52 **1.2.3 Save in binary compressed format**

53 Since haplotypes are long binary vectors, the entire haplotype reference panel can be compactly represented
54 using a single bit per entry. We have already divided the full reference panel into non-overlapping windows
55 of various widths after proper alignment of all typed and reference SNPs in the window. For each window we
56 save two compressed mini-panels. The first houses the unique haplotypes determined by just the typed SNPs.
57 The second houses the unique haplotypes determined by all SNPs in the window, typed or untyped. The
58 former is much smaller than the later, but each entry of both can be compactly represented by a single bit per
59 entry in memory. Thus, for each window we save two compressed windows in addition to meta information
60 and pointers that coordinate reference haplotypes with the two mini-panels per each window. This whole
61 ensemble is stored in the `jls` file. Because there are only a limited number of SNP array chips on the market,
62 one can in principle store just a few `jls` files on a universal source such as the cloud. The same JLSO
63 compressed panel can also be re-used as long as the set of typed SNPs does not change drastically between
64 different GWAS chips.

65 **1.3 Parallel Computing and Memory Requirements**

66 MendelImpute employs a shared-memory parallel computing model where each available core handles an
67 independent component of the entire problem. Work is assigned via Julia's multi-threading functionality.
68 When computing the optimal haplotype pairs in equation 1 of section 2.2, we parallelize over windows. This
69 requires allocating c copies of $\mathbf{X}^T \mathbf{H}$ and $\mathbf{H}^T \mathbf{H}$, where c is the number of CPU cores available. Note the

70 dimensions of these matrices vary across windows. To avoid accruing memory allocations, we pre-allocate
71 c copies of $n \times d_{max}$ and $d_{max} \times d_{max}$ matrices and re-use their top-left corners in windows with $d < d_{max}$.
72 For intersecting adjacent reference haplotype sets (phasing), we parallelize over samples. This step requires
73 no additional memory. Writing to output is also trivially parallelizable by assigning each thread to write a
74 different portion of the imputed matrix to a different file, then concatenating these files into a single output
75 file. Data import is not parallelized. Beyond allocating $\mathbf{X}^T \mathbf{H}$ and $\mathbf{H}^T \mathbf{H}$, our software requires enough memory
76 (RAM) to load the target genotype matrix and the compressed haplotype reference panel.

77 1.4 Bias Correction for Initializing Missing Data

78 Since BLAS requires complete data, we must first initialize the missing data in each genotype vector \mathbf{x} before
79 computing \mathbf{M} and \mathbf{N} in equation 2 of section 2.2. This may introduce bias in our minimization of equation 1 if
80 there is a high fraction of missing genotypes in the typed SNPs, for example above 10%. One way to alleviate
81 bias is to initialize missing data with the mean and save all unique haplotype pairs minimizing criterion
82 equation 1 under this convention. Once this set of optimal haplotype pairs are identified, we re-minimize
83 criterion equation 1 but now skipping the missing entries of \mathbf{x} . That is equivalent to setting $x_k - h_{ik} - h_{jk} = 0$
84 when x_k is missing.

85 1.5 Avoidance of Global Searches for Optimal Haplotype Pairs

86 Recall that minimizing equation 1 of section 2.2 requires searching through all lower-triangular entries of the
87 $d \times d$ matrix $\mathbf{M} + \mathbf{N}$, where d denotes the number of unique haplotypes in the window. When $d < 1000$,
88 searching through all $\binom{d}{2} + d$ lower-triangular entries of $\mathbf{M} + \mathbf{N}$ via MendelImpute’s standard procedure is
89 fast, but this global search quickly degrades as $d \rightarrow \infty$. Below we outline two heuristic procedures for large d .
90 These heuristics typically produce sub-optimal solutions compared to global searches, so they should be used
91 with caution.

92 1.5.1 Stepwise Search Heuristics

93 Consider minimizing the loss $f_i(\boldsymbol{\beta}) = \frac{1}{2} \|\mathbf{x}_i - \mathbf{H}\boldsymbol{\beta}\|_2^2$, where the d columns of $\mathbf{H} \in \{0, 1\}^{p \times d}$ store unique
94 haplotypes, p is the window width, and \mathbf{x}_i is a sample genotype vector. The original problem minimizes
95 $f_i(\boldsymbol{\beta})$ under the constraint that exactly two $\beta_j = 1$ and the remaining $\beta_k = 0$ or the constraint that exactly one
96 $\beta_j = 2$ and the remaining $\beta_k = 0$. As an approximate alternative, one first finds the r unique haplotypes with
97 the largest influence on $f_i(\boldsymbol{\beta})$. This is accomplished by identifying the r most negative components of the
98 gradient

$$\nabla f_i(\boldsymbol{\beta}) = -\mathbf{H}^T (\mathbf{x}_i - \mathbf{H}\boldsymbol{\beta}) = -\mathbf{H}^T \mathbf{x}_i + \mathbf{H}^T \mathbf{H}\boldsymbol{\beta}$$

99 at $\beta = \mathbf{0}$. These are the r directions of steepest descent. Note that $\nabla f_i(\mathbf{0}) = -\mathbf{H}^T \mathbf{x}_i$ and that $\mathbf{H}^T \mathbf{x}_i$ is pre-
 100 computed and cached in \mathbf{N} . The residual function $g_{ij}(\mathbf{h}_k) = \frac{1}{2} \|\mathbf{x} - \mathbf{h}_j - \mathbf{h}_k\|_2^2$ is then minimized over \mathbf{h}_k to
 101 find the candidate pair $(\mathbf{h}_j, \mathbf{h}_k)$ generated by each of the vectors \mathbf{h}_j determined by the gradient $\nabla f_i(\mathbf{0})$. The
 102 ingredients to perform these minimizations are already in hand. This heuristic scales as $\mathcal{O}(rd)$, much better
 103 than $\mathcal{O}(d^2)$ in the original formulation. MendelImpute sets the default $r = 100$. In the same spirit as the first
 104 step, one can alternatively find for each j the most negative component k of the gradient $\nabla f_i(\mathbf{e}_j)$, where \mathbf{e}_j is
 105 the standard unit vector with 1 in position j . This again determines a nearly optimal pair $(\mathbf{h}_j, \mathbf{h}_k)$. Under this
 106 tactic the Gram matrix $\mathbf{H}^T \mathbf{H}$ comes into play. Note that $\mathbf{H}^T \mathbf{H} \mathbf{e}_j$ reduces to its j th column \mathbf{v}_j . Hence, no new
 107 matrix-by-vector multiplications are necessary in calculating $\nabla f_i(\mathbf{e}_j) = -\mathbf{H}^T \mathbf{x}_i + \mathbf{v}_j = \nabla f_i(\mathbf{0}) + \mathbf{v}_j$.

108 Alternatively, one can find the best r unique haplotypes for a given sample \mathbf{x}_i *en masse* by arranging all
 109 pairwise column distances of \mathbf{X} and \mathbf{H} in the matrix

$$\mathbf{R} = \begin{bmatrix} \|\mathbf{x}_1 - \mathbf{h}_1\|_2^2 & \cdots & \|\mathbf{x}_n - \mathbf{h}_1\|_2^2 \\ \vdots & & \vdots \\ \|\mathbf{x}_1 - \mathbf{h}_d\|_2^2 & \cdots & \|\mathbf{x}_n - \mathbf{h}_d\|_2^2 \end{bmatrix}_{d \times n}.$$

110 Then we partially sort each column of \mathbf{R} to identify the top r haplotypes matching each sample \mathbf{x}_i . Here \mathbf{R}
 111 is computed via the `Distance.jl` package of Julia, which internally performs BLAS level-3 calls analogous
 112 to computing $\mathbf{H}^T \mathbf{H}$ and $\mathbf{X}^T \mathbf{H}$. Instead of searching through all haplotypes to minimize $g_{ij}(\mathbf{h}_k)$ for a given
 113 sample \mathbf{x}_i , one can instead search only over the $\binom{r}{2} + r$ combinations of the top haplotypes. This allows one
 114 to entertain much larger values of r . Empirically, choosing $r = 800$ works well for most data sets.

115 1.6 Phasing by Dynamic Programming

116 We also investigated a dynamic programming strategy that gives the global solution for minimizing the number
 117 of haplotype breaks across the extended haplotypes \mathbf{E}_1 and \mathbf{E}_2 . For each given haplotype pair $\mathbf{p}_1 = (\mathbf{h}_i, \mathbf{h}_j)$ in
 118 window w , we can compute the squared Hamming distance between it and the pair $\mathbf{p}_2 = (\mathbf{h}_k, \mathbf{h}_l)$ in window
 119 $w + 1$; in symbols

$$d(\mathbf{p}_1, \mathbf{p}_2) = \begin{cases} 0 & \mathbf{h}_i = \mathbf{h}_k, \mathbf{h}_j = \mathbf{h}_l & (0 \text{ breaks}) \\ 1 & \mathbf{h}_i = \mathbf{h}_k, \mathbf{h}_j \neq \mathbf{h}_l & (1 \text{ break}) \\ 1 & \mathbf{h}_i \neq \mathbf{h}_k, \mathbf{h}_j = \mathbf{h}_l & (1 \text{ break}) \\ 4 & \mathbf{h}_i \neq \mathbf{h}_k, \mathbf{h}_j \neq \mathbf{h}_l & (2 \text{ breaks}). \end{cases}$$

120 Observe that a double break is assigned an error of 4 to favor 2 single breaks across 3 windows as opposed to
 121 a double break plus a perfect match.

122 Now we describe a dynamic programming strategy for finding the two paths with the minimal number

123 of unique haplotype breaks. We start with all candidate pairs \mathbf{p}_i in the leftmost window and initialize sums
124 $s_i = 0$ and traceback path vectors \mathbf{t}_i to be empty. One then recursively visits all windows in turn from left to
125 right. If w is the current window, then every candidate haplotype pair \mathbf{p}_i in window w is connected to every
126 candidate pair \mathbf{p}_j in window $w + 1$. The traceback path \mathbf{t}_j is determined by the pair \mathbf{p}_k minimizing $d(\mathbf{p}_i, \mathbf{p}_j)$.
127 The traceback path \mathbf{t}_j is constructed by appending \mathbf{p}_k to \mathbf{t}_k and setting $s_j = s_k + d(\mathbf{p}_k, \mathbf{p}_j)$. This process is
128 continued until the rightmost window v is reached. At this point the pair \mathbf{p}_j with lowest running sum s_j is
129 declared the winner. The traceback path \mathbf{t}_j allows one to construct the extended haplotypes \mathbf{E}_1 and \mathbf{E}_2 in their
130 entirety. Unfortunately, too many haplotype pairs per window can overwhelm dynamic programming with
131 large reference panels because one must enumerate and store all possible haplotype pairs in every genomic
132 window for every individual. For large reference panels such as HRC, the number of possible haplotype pairs
133 often exceeds 100,000 per window. Thus, it is impossible to store all of these pairs in memory. One partial
134 recourse is to discard partial paths and associated partial termini \mathbf{p}_i that are unpromising in the sense that
135 their running sums s_i are excessively large. This does not completely alleviate the memory burden, and the
136 approximate algorithm is burdened by extra bookkeeping. The bookkeeping of the exact algorithm is already
137 demanding.

138 1.7 Msprime simulation script

```
139 # Usage: python3 msprime_script.py n ne seq recomb mut seed > full.vcf
140 # We used ne=10000; seq=10000000; seed=2020; recomb=2e-8; mut=2e-8
141 # n = 12000 or 102000 or 1002000
142
143 import msprime, sys
144
145 # parameters
146 sample_size = int(sys.argv[1])
147 effective_population_size = int(sys.argv[2])
148 sequence_length = int(sys.argv[3])
149 recombination_rate=float(sys.argv[4])
150 mutation_rate=float(sys.argv[5])
151 seed = int(sys.argv[6])
152
153 # run the simulation
154 ts = msprime.simulate(sample_size=sample_size, Ne=effective_population_size,
155 length=sequence_length, recombination_rate=recombination_rate, random_seed=seed)
156 model = msprime.InfiniteSites(msprime.NUCLEOTIDES)
```

Population Code	Description	Super Population
CHB	Han Chinese in Beijing, China	East Asian (EAS)
JPT	Japanese in Tokyo, Japan	East Asian (EAS)
CHS	Southern Han Chinese	East Asian (EAS)
CDX	Chinese Dai in Xishuangbanna, China	East Asian (EAS)
KHV	Kinh in Ho Chi Minh City, Vietnam	East Asian (EAS)
CEU	Utah Residents with NW European Ancestry	European (EUR)
TSI	Toscans in Italia	European (EUR)
FIN	Finnish in Finland	European (EUR)
GBR	British in England and Scotland	European (EUR)
IBS	Iberian Population in Spain	European (EUR)
YRI	Yoruba in Ibadan, Nigeria	Africans (AFR)
LWK	Luhya in Webuye, Kenya	Africans (AFR)
GWD	Gambian in Western Divisions in the Gambia	Africans (AFR)
MSL	Mende in Sierra Leone	Africans (AFR)
ESN	Esan in Nigeria	Africans (AFR)
ASW	Americans of African Ancestry in SW USA	Africans (AFR)
ACB	African Caribbeans in Barbados	Africans (AFR)
MXL	Mexican Ancestry from Los Angeles USA	Ad Mixed American (AMR)
PUR	Puerto Ricans from Puerto Rico	Ad Mixed American (AMR)
CLM	Colombians from Medellin, Colombia	Ad Mixed American (AMR)
PEL	Peruvians from Lima, Peru	Ad Mixed American (AMR)
GIH	Gujarati Indian from Houston, Texas	South Asian (SAS)
PJL	Punjabi from Lahore, Pakistan	South Asian (SAS)
BEB	Bengali from Bangladesh	South Asian (SAS)
STU	Sri Lankan Tamil from the UK	South Asian (SAS)
ITU	Indian Telugu from the UK	South Asian (SAS)

Table 1: The 26 population codes present in the 1000 genomes project.

```

157 ts = msprime.mutate(ts, rate=mutation_rate, model=model, random_seed=seed)
158
159 # print results (2 is for diploid, "legacy" = no matching positions)
160 with sys.stdout as vcffile:
161     ts.write_vcf(vcffile, 2, position_transform="legacy")

```

1.8 Summary of 1000 Genomes Reference Panel

A total of 26 different populations contribute to the 1000 Genomes Project data set. These populations are further organized into five super population. While this information is freely available online, we summarize it in Table 1 for completeness.

166 **2 Author contributions**

167 KL, JS, ES, and HZ conceived this project. BC, KL, RW, JS, ES, and HZ devised the methods. BC, RW, and
168 HZ developed the software. S.K added BGEN support. BC and KL accessed the data. BC wrote the original
169 draft of the paper. BC, KL, RW, JS, ES, and HZ reviewed and edited the draft. KL previewed some of the
170 methods incorporated in MendelImpute in his talk [3].

171 **3 Acknowledgements**

172 BC and RW were supported by NIH grant T32-HG002536. BC, ES, JS, HZ, and KL were supported by
173 NIH grant R01-HG006139. ES, JS, HZ, and KL were supported by NIH grant R01-GM053275. JS was also
174 supported by NIH grant R01-HG009120.

175 We would also like to thank Calvin Chi for his helpful discussions on ancestry estimation and Juhyun Kim
176 for her helpful discussions on imputation quality scores.

177 **4 Competing interests**

178 The authors declare no competing interests.

179 **5 Web Resources**

180 **Project name:** MendelImpute.jl

181 **Project home page:** <https://github.com/OpenMendel/MendelImpute.jl>

182 **Supported operating systems:** Mac OS, Linux, Windows

183 **Programming language:** Julia 1.6

184 **License:** MIT

185 All commands needed to reproduce the following results are available at the MendelImpute site in the
186 manuscript sub-folder. SnpArrays.jl is available at <https://github.com/OpenMendel/SnpArrays.jl>.
187 VCFTools.jl is available at <https://github.com/OpenMendel/VCFTools.jl>. The Haplotype Ref-
188 erence Consortium data is available at <https://www.ebi.ac.uk/ega/datasets/EGAD00001002729>. Raw
189 1000 genomes data is available at <ftp://ftp.1000genomes.ebi.ac.uk/vol1/ftp/release/20130502/>,
190 and Beagle's webpage http://bochet.gcc.biostat.washington.edu/beagle/1000_Genomes_phase3_v5a/
191 v5a/ provides a quality controlled 1000 genomes data which we used in our experiments.

192 **References**

- 193 [1] R. Finnegan and L. White. invenia/JLSO.jl: Storage container for serialized Julia objects. [https://doi.](https://doi.org/10.5281/zenodo.3992374)
194 [org/10.5281/zenodo.3992374](https://doi.org/10.5281/zenodo.3992374), 2020.
- 195 [2] A. GreenWell and M. Abbott. GroupSlices.jl: A package for the groupslices and associated functions.
196 <https://github.com/mcabbott/GroupSlices.jl>, 2019.
- 197 [3] K. Lange. Lecture on Ultrafast Haplotyping. In *New Statistical Methods for Family-Based*
198 *Sequencing Studies*. Banff International Research Station, [http://www.birs.ca/events/2018/](http://www.birs.ca/events/2018/5-day-workshops/18w5154/videos/watch/201808091354-Lange.html)
199 [5-day-workshops/18w5154/videos/watch/201808091354-Lange.html](http://www.birs.ca/events/2018/5-day-workshops/18w5154/videos/watch/201808091354-Lange.html), 2018.
- 200 [4] E. Y. Liu, M. Li, W. Wang, and Y. Li. MaCH-Admix: genotype imputation for admixed populations.
201 *Genetic Epidemiology*, 37(1):25–37, 2013.